Fall 2020

Quantification of Neurite Degeneration through use of an Optimized and Automated Method

Lauren Fuller
Eastern Kentucky University, lauren_fuller7@mymail.eku.edu

Eastern Kentucky University

Quantification of Neurite Degeneration through use of an Optimized and Automated Method

Honors Thesis

Submitted

In Partial Fulfillment

Of The

Requirements of HON 420

Fall 2020

By

Lauren Fuller

Faculty Mentor

Dr. Bradley Kraemer

Department of Biological Sciences

Quantification of Neurite Degeneration through use of an Optimized and Automated Method

Lauren Fuller

Dr. Bradley Kraemer
Department of Biological Sciences

Abstract

Neurite degeneration is a cellular dysfunction commonly associated with neurodegenerative pathologies such as Alzheimer's disease and Parkinson's disease (PD). One common method of scoring neurite degeneration in micrographs involves calculation of a degeneration index (DI) using neurite fragment measurements obtained via the particle analyzer plugin of FIJI software. However, this method can be time consuming and subject to inaccuracies related to inadequate contrast. Here we describe a modified method for performing DI measurements with enhanced efficiency, accessibility, and accuracy compared to existing techniques. We developed a macro to automate the analysis process, enabling rapid and objective measurements of multiple images. We have also increased the accuracy of measurements by modifying selection criteria for neurite fragments, as well as by determining optimal procedures for contrast enhancement and removal of non-neurite materials from images. Moreover, we demonstrate how this method may be applied to measure neurite degeneration in an *in vitro* model of PD. To model neurite degeneration associated with PD, we treated Lund Human Mesencephalic (LUHMES) cells with 4-hydroxynonenal or 6-hydroxydopamine, compounds that induce oxidative stress. We describe culture methods, cell densities, and

drug concentrations that yield consistent and accurate measurements of neurite degeneration, and we demonstrate use of our optimized method in an experiment assessing the effects of c-Jun N-terminal Kinase (JNK) on neurite degeneration. Since neurite degeneration is a key, early-stage event associated with PD, this optimized and automated method may be used to gain novel insights into molecular interactions underlying PD progression.

Keywords and phrases: neurite degeneration, neurite, Parkinson's Disease, fragmentation, neurodegeneration, degeneration index, D.I., quantification, FIJI, particles

Table of Contents

List of Figures

Acknowledgments

First and foremost, I would like to extend my gratitude to Dr. Bradley Kraemer for mentoring me and allowing me to conduct research in his lab. He encouraged me to grow as someone who greatly values knowledge and learning. Most importantly he helped me grow as a scientist, teaching me the precious lesson of having cautious optimism. I would also like to thank my lab-mates Rachel Clements, Wesley Hall, and Jeanne Reix Charat for helping to contribute to the 6-OHDA, HNE and SP600125 data for the corresponding figures. I would also like to thank the EKU Honors Program for allowing me to research and present my own work. Above all, I would like to give appreciation to my family and friends who have supported me throughout the whole thesis process. Specifically, I would like to thank my mom, Dena, my dad, Jay, my sister, Heather, my children Tyson and Kali, and my cousin, Deven. I would also like to thank all my other loved ones for supporting me along the way.

Introduction

Neurodegeneration

Neurodegenerative disorders are becoming a more common issue as lifespan has become extended. Currently, these diseases are incurable. However, there has been an increased interest in understanding these disorders so that more novel therapies may be developed (Heemels, 2016). Some examples of these type of illnesses are Alzheimer's disease (AD), Parkinson's Disease (PD), Huntington's disease, amyotrophic lateral sclerosis (ALS), Multiple sclerosis (MS), and dementia. The pathophysiologies of these disorders are specific. However, in each case there is the progressive degeneration of neurons. Depending on the circumstance, this type of degeneration may result in cognitive impairment, issues relating to memory, and deficits in motor function. (Gitler et al. 2017).

Neurons are the cells of the nervous system and they are responsible for receiving sensory input from the external environment and are also responsible for sending motor impulses to the muscles of the body, allowing for movement and everyday functioning. The neuron is composed of three main parts: the soma (cell body), dendrites, and axon. The cell body of the neuron is the spherical center of the cell that contains the nucleus and specialized organelles of the cell, and this area acts as a control center where electrical and chemical impulses are processed. Dendrites are projections from the soma that are responsible for receiving chemical signals from other nearby neurons. The axon is a single long tail-like projection off of the other side of the soma that is responsible for transmission of an electrical impulse known as an action potential. The axon end may have several branches itself so that it may innervate multiple nearby neurons or target

cells. Axons of the central nervous system are commonly covered in what is known as a myelin sheath. This is a fatty white coating that surrounds the axon and acts as an insulator, allowing for increased speed of transmission of impulses. The myelin sheath is broken up into segmented parts clustering sodium channels at myelin-free interspaces—the nodes of Ranvier—to enable saltatory action potential conduction (Ettle et al. 2016). Collectively the dendrites and axon of a neuron are called neurites, these specific structures may become degenerated/fragmented at the onset of neurodegenerative diseases.

The destruction of neurites poses a problem because they are essential for neuronal communication and nervous system functioning. Neurons communicate using action potentials, which is the occurrence where there is a brief reversal of the electrical polarization of a neuron's membrane. The occurrence of an action potential is what allows for an electrical signal to travel down and through the neuron. Normally neurons, when at rest, have a negatively charged internal environment due to the balance of potassium and sodium ion concentrations inside and outside of the cell. This concentration is established by the Na^+/K^+ -ATPase pump. This is a transmembrane protein that moves three sodium ions out and two potassium ions in with each pump. This sets up a concentration where the inside of the cell is negative compared to the outside environment.

There may then be a depolarizing event initiated by a stimulus that can trigger an action potential through the neuron. This is an electrical signal that travels down the axon towards the axon terminal and synapse. During depolarization sodium gated ion channels open and sodium floods into the cell and this causes a local change in potential that gets

propagated down the axon. Once an action potential reaches the terminal the electrical signal induces a localized rise is calcium ion concentration within the cytosol that triggers the release of neurotransmitters from vesicles into the synaptic cleft. The neurotransmitter will then bind to receptors on the target cell leading to changes in excitability of the postsynaptic cell (Lodish et al. 2000). Once depolarization has occurred, there is repolarization and hyperpolarization of the cell, where sodium channels close and voltage gated potassium channels open to reestablish the resting membrane potential, until another stimulus triggers an action potential once again.

The structural integrity of neurites is maintained by three different cytoskeletal filaments that allow for changes in cellular morphology. The filaments are microtubules, microfilaments, and intermediate filaments. Through interaction of these protein classes with each other, other proteins and different cellular membranes, the cell develops a defined shape and structure (Flynn 2013). Neurite fragmentation is an early stage event that occurs with the onset of neurodegenerative disorders, normal physiology is associated with healthy, intact neurites. However, with certain pathologies neurites become fragmented and have a negative impact on signaling between cells. As described, neurodegenerative diseases can have a large impact on neuron structure and cognitive and motor skills.

Neurodegenerative Diseases

Two of the most well-known examples of neurodegenerative diseases are Alzheimer's disease (AD) and Parkinson's disease (PD). Though there are some similarities among these two diseases, they are different when it comes to symptoms and their overall physiology. AD presents with symptoms of memory loss, confusion, issues

with language, poor judgment, and the inability to learn new information. Many times, the onset of AD is slow and subtle. There may be small lapses in memory, and this may be diagnosed as mild cognitive impairment (MCI). However, as the disease progresses symptoms can become increasingly worse and eventually may be debilitating. Typical duration of the disease until death is 8-10 years, and Alzheimer's is the sixth leading cause of death in the United States (Rosenthal and Kamboh 2014).

Clinical assessments of AD patients reveal the accumulation of β-amyloid plaques and intraneuronal neurofibrillary tangles that contain tau protein. These plaques and tangles interfere with calcium signaling and synaptic transmission. This brings about a constant state of inflammation and leads to neuronal death. Neurons in the part of the brain responsible for memory, the hippocampus, become damaged in AD. The entorhinal cortex, the area of the brain that functions as a hub in a widespread network for memory, navigation and the perception of time, also degenerates in AD. Neuroimaging also reveals that there is cerebral cortical atrophy present in AD patients (Bird 2018). With the deposit of β-amyloid plaques there comes neurite degeneration that may occur. These neurites present as being dilated and tortuous, and often have other structural changes that affect organelles. For example, these dystrophic neurons may have enlarged lysosomes and numerous mitochondria (Selkoe 2001). There are various theories regarding why a patient develops AD, but one that many scientists and doctors can agree upon is that AD is linked to genetics. Some reports present up to a 50% genetic link to the development of AD. It may be difficult to directly link AD genetically because many times polymorphic alleles may predispose someone to AD, but not exclusively cause the onset of the disease.

There are two main categories of AD, early-onset (EOAD) and late-onset (LOAD) so that further complicates research. Mutations in three genes, including amyloid precursor protein (APP), presenilin (PS)-1 and PS-2, have been linked to EOAD. This is promising, but the majority of AD cases are LOAD where patients develop symptoms when they are sixty years old or older. There has been a link between the ε4 allele of apolipoprotein E (*APOE*) and the development of LOAD. APOE is a protein that commonly gets combined with lipids in the body to form lipoproteins that are then used for packaging and carriage of other fats through the bloodstream. Having the ε4 allele is a major genetic risk factor of LOAD, but the exact mechanism in which it influences development of the disease is still unknown (Rosenthal and Kamboh 2014).

Parkinson's Disease (PD) is the second most common neurodegenerative disease in the United States, affecting around 1 million people. PD symptoms include bradykinesia, rigidity, tremor, and postural instability. Motor incoordination is a hallmark of PD, but the disease also can have an effect on memory and mood (McDonald et al. 2003). Most patients are diagnosed with PD between 55-66 years of age. With the onset and progression of PD there is the build-up of Lewy bodies. Lewy bodies are clumps/deposits of the α-synuclein protein. This can cause issues with signaling and motor movement (Stroud et al. 2013).

A distinctive feature of PD is the degeneration of dopaminergic (DA) neurons in the substantia nigra pars compacta (SNc) brain region. Dopaminergic neurons are nervous system cells that produce dopamine (DA). The SNc area of the brain is connected to the striatum in the forebrain, which is associated with motor systems. At the clinical onset of PD there is only a 30% loss of total substantia nigra pars compacta

neurons, but there is 70-80% loss of striatal dopaminergic markers which suggests that axon terminals (ends of neurites) are affected earlier. With overexpression of the α-synuclein protein there is a significant decrease in the number of motile vesicles and there is decelerated vesicle transport affecting transmission of neurotransmitter (Koch et al. 2015). Studies have shown that transplantation of embryonic dopaminergic neurons have improved the symptoms and reinnervation of neurons in some patients with severe PD (Freed et al. 2001). PD may also be familial and mutations in certain genes and exposure to environmental toxins may lead to mitochondrial dysfunction, another hallmark of PD. When cells are exposed to stress linked to PD progression, there is the dual event of accumulation of α-synuclein protein and mitochondrial dysregulation that occurs (Scorziello et al. 2020). PD also has a genetic linkage. Neuronal death has been linked to mutations in these PD-related genes: *SNCA*, *LRRK2*, *DJ-1, PARK2*, *PINK-1* (Trist et al. 2019). Non-genetic factors that may bring upon the onset of PD include occupational exposure to toxins and heavy metals (Salari and Bagheri 2018). Neurodegeneration can occur in many forms. Some diseases target the cell body, or the axons and dendrites independently. The goal of this research is to investigate neurite degeneration, in order to give an accurate, efficient, and more user-friendly method to quantify this type of degeneration.

Neurite Degeneration

Neurite degeneration can occur in a variety of ways. For example, there may be fragmentation or blebbing that occurs. Fragmentation involves the neurite, after exposure to stress, beginning to break up into smaller fragments, which poses an issue with impulse transmission. Blebbing refers to protrusions of the plasma membrane of a cell

that acts as an early cytotoxic event. This is due to reorganization of the cytoskeletal proteins (Lesort et al. 1997). Visually when a neuron begins to bleb, it appears as though the neurite begins to swell in certain areas.

Fragmentation and blebbing are two broad categories of degeneration, but there are specific conditions that involve these mechanisms in the degradation process. One example would be Wallerian degeneration (WD). This type of deterioration relates specifically to axons. When an axon is injured (axotomy) it immediately separates from the soma and then actively executes its own destruction. After an axon has separated from the soma it has a lag phase where there is no change in morphology and then it will begin to disassemble in the way of granular fragmentation distal to the site of injury. Surrounding glial cells clear away axonal debris and then the process of axonal regeneration to reestablish connectivity occurs (Llobet and Neukomm 2019). WD is important for development of a neuronal network and axonal pruning. When degeneration occurs first at locations distal to the cell body, it occurs in a “dying-back fashion”. Depending on the injury and type of disease the soma may stay healthy and intact or it may also begin to deteriorate (Yaron and Schuldiner 2017).

Neurite degeneration may also include loss of myelin sheath on the axon. This may not directly fragment the neurite itself, but it may affect the speed of transmission along the neurite. The cells that compose the myelin sheath are known as oligodendrocytes and Schwann cells. Oligodendrocytes produce myelin and wrap multiple axons of the central nervous system, and they also provide metabolic and trophic supply to help maintain neuron function (Ettle et al. 2016). Schwann cells act in the same way, but they are located in the peripheral nervous system and they only wrap one axon

at a time. With the neurodegenerative disease MS specifically, there is loss of myelination of the axon, presenting as a type of neurite degeneration. Depending on the location of the demyelination, there can be issues with walking and balance dysfunction (Kim et al. 2020). This type of neurite degeneration does not occur in PD since the neurons of the substantia nigra are not myelinated (Sulzer and Surmeier 2012). Many times, neuronal death and injury occurs in response to oxidative stress and interactions with reactive oxygen species.

Oxidative Stress / ROS

When discussing cellular dysfunction, exposure to oxidative stress and reactive oxygen species (ROS) plays a critical role in the onset and progression of neurological pathologies. Oxidative stress is cellular condition in which there is the imbalance of ROS and naturally occurring antioxidants. ROS are generated during aerobic metabolism, and these are highly chemically reactive transient species that contain oxygen that may form adducts with and interact with DNA, proteins, carbohydrates, and lipids in a destructive manner. Oxygen has a high electron affinity. ROS may include free radicals like the superoxide anion (O_2^-), hydroxyl radicals (-OH) and the nonradical hydrogen peroxide (H_2O_2). Free radicals are uncharged molecules that have an unpaired valence electron. Due to this reason, they are extremely reactive and can cause damage to cells via oxidation. This is the process of loss of electrons. In this situation an ROS may interact with a macromolecule and “steal” one of its electrons, causing cellular dysfunction. Not all ROS are considered free radicals, but they can cause degeneration nonetheless (Curtain et al. 2002). Mitochondrial production of ATP, inflammation, and phagocytosis are endogenous processes that may produce ROS. Mitochondria produce ATP through

oxidative phosphorylation. Many times, the mechanisms that remove damaged mitochondria are altered in PD systems. This is an autophagy process that is specifically called mitophagy. If there is this type of alternation there may be accumulation of damaged mitochondria that may lead to oxidative stress and irreversible apoptotic cell death (Scorziello et al. 2020). Oxidative stress is present in other neurodegenerative disorders and this may be due to the fact that the central nervous system is a highly aerobic environment that requires a high energy source and mitochondrial function, so it is more susceptible to this particular kind of stress. The brain requires 20% of body basal oxygen to function (Cenini et al. 2019). Environmental sources such as exposure to x-rays, ozone, cigarette smoking, air pollutants, and industrial chemicals may also cause formation of ROS and other free radicals (Lobo et al. 2010).

Oxidative stress may induce cell death via necrosis or apoptosis. Necrosis occurs usually in response to severe trauma to the cell. Morphological changes present as cytoplasmic and mitochondrial swelling, plasma membrane rupture and release of the cellular contents into the extracellular space. Induction of the immune response to clean up cellular debris may cause even more death to neighboring cells. Apoptosis is programmed cell death and this function is much more tightly regulated. The cell begins to depolarize and fragment into what are called apoptotic bodies (Curtain et al. 2002).

Cells within the body naturally have antioxidant defenses but as there is an increase of ROS and free radicals there may be an imbalance that leads to oxidative stress. Diet may introduce additional antioxidants to help combat this issue. Antioxidants work by directly scavenging ROS and providing them with a free electron. Some examples of antioxidants obtained from diet are β-carotene, vitamin C and vitamin E.

Foods that are rich in antioxidants include berries, cherries, citrus, prunes, and olives. Green and black teas are also a great source of antioxidants (Lobo et al. 2010).

In relation to PD, there is evidence of increased ROS presence in the substantia nigra region of postmortem brains of PD patients (Cenini et al. 2019). In many cases, in order to research and properly model PD, investigators will use drugs that will chemically induce oxidative stress. One of the most popular toxins that induces neurite degeneration is 6-hydroxydopamine (6-OHDA). This is a synthetic organic compound that promotes the select degeneration of DA neurons. The chemical structure of 6-OHDA is very similar to the chemical structure for DA, apart from a hydroxyl group attached to the sixth carbon of the ring. This is important to note since it is brought into the neuron via dopamine reuptake transporters. 6-OHDA has been shown to disrupt complex I of the mitochondrial electron transport chain as well as increase production of ROS, which contribute to neuronal death via apoptosis. Molecules of 6-OHDA may even combine to form quinones, a type of ROS. In one study, use of 6-OHDA immediately saw the dysfunction of mitochondrial transport, and this event was blocked by use of the anti-oxidant N-acetyl-cysteine (NAC) suggesting that free radical species played a role in this process (Lu et al. 2014). This type of degeneration may present as axonal blebbing and fragmentation. Another drug used to chemically induce PD is 1-methyl-4-phenyl-1,2,3,6-tetrahydropyridine (MPTP). This compound also selectively kills DA neurons and has been linked to immune system depression (Basu and Dasgupta 2000).

Fragmentation of neurites may also occur experimentally after exposure to 4-hydoxynonenal (HNE). This is a byproduct of lipid peroxidation. This is the event where the lipid membrane of a cell is oxidized. HNE may form covalent adducts with

macromolecules and disrupt their function (Zhong and Yin 2014). HNE can induce inflammation and trigger apoptosis. HNE preferentially forms adducts with cysteine residues of thiol-containing proteins, a number of which are proteins involved in redox signaling (electron transfer reactions). Thiol groups are organic compounds that have the form R-SH, so they are very similar to alcohols, but there is a sulfide instead of an oxygen. One such protein that HNE may interact with is c-Jun N-terminal kinase (JNK) (Breitzig et al. 2016). This is a protein associated with stress signaling pathways. These pathways may be triggered with exposure to cytokines, growth factors, and oxidative stress. JNK is activated via phosphorylation. These signaling pathways have been shown to have a key effect on apoptosis signaling. In relation to AD, JNK proteins have been reported to increased amyloid beta production and contribute to the development of neurofibrillary tangles (Yarza et al. 2016). When it comes to PD, JNK protein blockage has also been shown as an effective way to alleviate oxidative stress brought on by other neurotoxic drugs (Wang et al. 2004). One way to block JNK is through the use of an inhibitor such as SP600125, a chemical used to block phosphorylation. The concept of oxidative stress is important in relation to PD because many times there is the induction of oxidative stress within cell cultures in order to model and research PD.

Parkinson's Disease

Parkinson's patients experience degeneration of dopaminergic neurons specifically. These neurons produce dopamine, which is a neurotransmitter and hormone with many important functions. It primarily is associated with motor coordination and motivation. DA is produced in the substantia nigra, ventral tegmental area, and hypothalamus of the brain. It is made from the conversion of the amino acid tyrosine into

levodopa (L-dopa) via the enzyme tyrosine hydroxylase (TH). Presence of this enzyme indicates presence of DA neurons. The L-dopa compound then undergoes an enzymatic process to become dopamine. This specific neurotransmitter acts as a precursor itself to other neurotransmitters like epinephrine and norepinephrine, so degeneration of DA may also have an effect on sleep, dreaming, mood, attention, working memory, and learning. Degeneration of DA neurons is not only limited to PD patients. On average there is a 5-10% decrease of overall DA neurons with every decade of life as there is an increase in brain oxidative damage relating to aging (Olguin et al. 2015).

DA neurons are susceptible to oxidative stress and degeneration due to their negative mitochondrial membrane potential. When treated with MPTP, the DA neurons of primates and mice saw degeneration due to MPTP's metabolite MPP+ concentrating in the mitochondria. Similar to 6-OHDA, MPP+ is also uptaken into the DA transporter (DAT). Another theory as to why DA neurons are more vulnerable to degeneration relates to energy production. Axons of the SNc are not myelinated which may mean they have a decreased abundance of substrates to support ATP production. This can pose an issue because if DA neurons are intrinsically more energetically challenged then they might be predisposed to mitochondrial insults (Haddad and Nakamura 2015). Other factors like calcium, iron dysregulation and antioxidant deficiencies may also affect the neuronal redox balance which may make DA neurons more susceptible to degeneration as a person ages.

In individuals with PD, the DA neurons of the substantia nigra brain region become degenerated. This area of the brain is located in the mesencephalon (midbrain). This brain region is a basal ganglion structure, meaning it is linked to the thalamus at the

base of the brain and it is involved in coordination of movement and reward. The term substantia nigra means “dark substance” due to the high neuromelanin content which forms from the L-dopa precursor in dopamine synthesis (Sonne et al. 2020). This section is made up of two subsections called the substantia nigra pars compacta (SNc) and the substantia nigra reticulata (SNr). The two sections lie medially to each other. The neurons of the SNc are very densely packed and reach the striatum (a structure in the forebrain) and supply it with dopamine. The striatum is associated with fine motor movements and action planning. The neurons of the SNr project out and are considered to be GABAergic, meaning they release Gamma aminobutyric acid (GABA), an inhibitory neurotransmitter, so it blocks impulses between nerve cells. The SNr as a whole contributes to seizure suppression (Zhou and Lee 2011). Neurons of the SNc often begin to degenerate first at the ends of the neurites and then progress in a dying back fashion (Grosch et al. 2016). Once PD presents symptoms clinically there is already substantial loss of DA neurons between the SNc and the striatum.

There are three major dopamine pathways that Parkinson’s is related to, the mesolimbic, mesocortical and nigrostriatal pathways. The mesolimbic pathway is often referred to as the reward pathway as it mediates pleasure signaling. It connects the ventral tegmental area (VTA) in the midbrain to the ventral striatum of the basal ganglia in the forebrain. This is a connection that goes to parts of the limbic system, which is a set of structures associated with motivation, emotion, learning, and memory. The VTA specifically is a group of neurons near the midline of the brain that acts as the origin of DA cell bodies for these pathways. The mesocortical pathway runs from the VTA to the cerebral cortex- the thin layer of the brain that covers the cerebrum. The cerebrum is the

largest part of the brain that spans from the frontal bone to the occipital bone. The cerebral cortices' main functions are associated with attention, perception, awareness, thought, memory, language, and consciousness. The purpose of this pathway is to regulate cognitive control, motivation, and emotional response (Luo and Huange 2016). Pathologies of this pathway may include schizophrenia. This type of disorder results from an excess of DA. The final pathway is known as the nigrostriatal pathway. This pathway connects the SNc with the dorsal striatum in the forebrain. Neurons in the SNc synapse on and release DA onto GABAergic neurons of the striatum. With the combined presence of DA and GABA neurotransmitter there is the induction of voluntary fine motor control within basal ganglia circuitry/motor loops (Bourdy et al. 2014). DA neurons of the nigrostriatal pathway have a higher basal rate of mitochondrial oxidative phosphorylation and ATP production and a smaller reserve capacity compared to less vulnerable DA neurons of the VTA, relating to the mesocortical and mesolimbic pathways. Neurons in the nigrostriatal pathway seem to also be more vulnerable due to complex axonal arborization; this is the process of development of tree-like branching that occurs (Giguere et al. 2019).

Dopamine interacts with many parts of the brain, but it is not the only neurotransmitter affected by PD. Patients with PD may also present with secondary mood-related symptoms in addition to motor impairment. Many times, PD patients also have issues with depression and anxiety related to the neurotransmitter serotonin. The area of the brain known as the raphe nuclei (RN), located in the brainstem, is responsible for production and release of serotonin and with early stages of PD there is Lewy body pathology that presents in this area. There is a reported loss of 56% of serotonergic

neurons in the median RN area of PD patients. This loss was correlated with depression in PD patients (Grosch et al. 2016). This relates to data from actual PD patients, but when studying neurodegeneration that presents in PD in a research setting, most data comes from animal models. There is a multitude of previous literature and research that can be drawn upon, but each source may vary in techniques and experiments used.

Studying PD in a Research Setting

Parkinson's disease may be modeled in a research setting using cell culture lines of DA neurons or it can also be modeled by working with tissue samples taken from test rodents. This relates to the difference between primary and secondary cell culture. Primary cell culture involves dissection and dissociation of cells from animal or plant tissue directly through mechanical or enzymatic processes and then maintaining growth of those cells in a suitable outside environment. These cells may easily be contaminated with mycoplasma (a type of bacteria) so in many cases they may be treated with antibiotics (Geraghty et al. 2014). Secondary cell culture involves taking cells from the primary culture and putting them into a new vessel with fresh growth media. This enables longer lifespans of the cells and the opportunity for expanding cell populations. One thing to note is that secondary culture may invariably cause genetic changes from the original primary culture. In our experiments we use secondary cell culture.

In research settings PD may be modeled chemically by use of certain drugs that induce oxidative stress, or it may be modeled genetically. This is where an investigator might bring about the onset of PD by disrupting genes associated with the disease. Most commonly PD is modeled chemically by use of 6-OHDA injected intracranially (Taherianfard et al. 2020). Other investigators may choose to manipulate genes

associated with PD to induce the same type of Parkinsonism symptoms. These specific genes may be targeted for mutation to generate “knockout” mice/rats. Most commonly there are three genes, PINK1, Parkin and DJ-1, that if manipulated to induce loss-of-function will result in recessively inherited PD onset. Gain-of-function single point mutations in the LRRK2 and α-synuclein genes have been linked to dominantly inherited PD. When inducing PD genetically in animal models, it has been suggested that rats may be a better option than mice to investigate. This is because mice that are genetically manipulated show no greater than 50% nigral DA neurons. However, rat genetic models routinely produce greater than 50% nigral DA neuronal cell loss, most similar to human onset of PD (Creed and Goldberg 2019). Though it is obvious that PD has been heavily researched, there are some techniques that specifically are used when investigating neurite degeneration.

In a broader sense, PD can be modeled using cell culture, which is a type of *in vitro* representation, or it may be modeled *in vivo*. The difference is where experimentation is occurring. *In vivo* studies investigate cells in their native conditions and *in vitro* studies have removed the cell from its natural environment and it is placed in an artificial environment that mimics natural biological conditions. For *in vivo* studies of PD, rodents such as mice and rats are commonly used to model human patients. One common approach involves the stereotaxic injection of oxidative stress inducing drugs (like 6-OHDA) into the medial forebrain of the animal. The word stereotaxic refers to a three-dimensional surgical technique that allows for areas deep within tissue to be treated chemically. With the intracranial injection of 6-OHDA there may be death of up to 60% of tyrosine-hydroxylase containing neurons (Salari and Bagheri 2018).

Our research makes use of experimentation with cells from the Lund human mesencephalic (LUHMES) cell line. These cells are derived from 8-week-old human mesencephalon embryonic tissue. In order to immortalize the cells, DNA from a cancer gene called v-myc was introduced to encourage rapid division. This gene is near a tetracycline-controlled promoter, so inactivation of the v-myc gene may occur if the cells are treated with tetracycline, a type of antibiotic. Once these cells have been treated with tetracycline they develop into post-mitotic neurons and develop a neuronal network as their neurites begin to flourish morphologically. This process is called differentiation. In addition to tetracycline, differentiation media also includes glial cell-derived neurotrophic factor (GDNF) and dibutyryl-cyclic AMP (db-cAMP). GDNF is a protein that promotes survival of neurons and db-cAMP signaling pathway activation is required for GDNF to have positive impact on the neurons. In one study combined treatment of mesencephalic cultures with db-cAMP and GDNF accelerated the onset of the survival effects of GDNF on dopaminergic neurons, resulting in a 1.5-fold increase in the number of surviving TH neurons at 3 days *in vitro* (Engele and Franke 1996). These cells are used in modeling PD because they express dopaminergic neuron specific markers. These cells may be treated with stress inducing drugs and then different aspects of their degeneration may be measured. Analysis of protein before and after treatment may occur via western blot analysis or by use of immunostaining. Neurite degeneration may be visualized using microscopy to see axonal blebbing or fragmentation (Zhang et al. 2014).

Previous Research of PD

Degeneration of a neuron may present in many different ways. For example, there can be degeneration of the soma, loss of myelination, blebbing or fragmentation of

neurites. In our research we want to evaluate deterioration of the neurites in a fragmented manner. Several methods for measuring neurite degeneration have been previously reported. These methods may be put into two categories: automated and manual methods. Both may make use of imaging software, for example, ImageJ or the new modified version of this program, FIJI.

One team of investigators chose to investigate how human nerves in the peripheral nervous system (PNS) degenerated via counting axon tracts with manual, semi-automated and automatic methods. They did so by taking nerve biopsies of patients with facial palsy. This is a condition that also goes by the name of Bell's palsy, and it is characterized by the paralysis of facial muscles on one side of the face, due to dysfunction of the facial cranial nerve. In this study grayscale micrographs of the nerve fascicules (bundle of axons in the PNS) were acquired and processed using FIJI software. This team made use of tools in FIJI to trace and cut the cross-section image of the sample, and manual counts of the axons were performed by an independent blinded examiner. This method examined the axon count as a way to measure degeneration present in facial palsy patients. This was in contrast to their semi-automatic counts where they used a function of FIJI to analyze and detect particles of a certain size to count the axons automatically. This version of the method was not fully automated because additional steps were done manually in order to increase the contrast of the starting images. These steps included increasing the contrast and then binarizing the image. Binarization of the image means to convert it into black and white so that the neuron structure is black upon a white background. This concept is related to "thresholding" an image, where pixels are divided into two or more classes. In this situation the two classes

are the “background” and “foreground” of the image. The team fully automated the method by use of a macro in FIJI. Macros are lines of script within the software that allow for simultaneous application of separate and numerous modifications to whole image sets. The time difference between manual and automated methods was astounding, as the manual method for 129 biopsies took 21 hours and 6 minutes, when in comparison the semi-automated method only took 1 hour and 47 minutes (Engelmann et al. 2020).

Other studies investigate length of neurite outgrowth as a way to quantify degeneration. One example relates to the work of a team of experimenters that demonstrated the quantification of axonal degeneration present in dorsal root ganglia (DRG) due to the withdrawal of the neurotrophin Nerve Growth Factor (NGF). The DRG is a ganglion (a group of neurons within the PNS) that is located within the dorsal root of the spinal nerve. In their experiments they introduced a way to measure axonal density over an entire field of radial outgrowth from the ganglion. *In vivo* DRG axons connect other peripheral tissues to spinal tissue. DRG also respond positively to NGF, which binds to receptors on growing DRG axons and initiates a pro-growth and pro-survival signaling cascades. Neurons that reach their target flourish, but those that do not degenerate (Johnstone et al. 2018). Instead of using an *in vivo* model, the researchers used explant DRG–transferred from animals to a nutrient media– and measured axonal degeneration from micrographs using Axoquant 2.0 in R studio. This program (Axoquant 2.0) was created by the authors and is an R script (text file in the programming language R). This program gets opened in R Studio. R Studio is a graphical interface for editing and running R packages. This tool avoids variations in random sampling of neurons by instead reporting the degree of degeneration over the entire radial growth field from the

soma to the growth cone. A growth cone is a large actin supported extension of a growing neurite seeking its synaptic target. Results are reported as distance from the soma x area occupied by the axons. One strength of this experiment is that it is not prone to any type of bias since it is not relying on random sampling, and it is not dependent on the researcher's decision of whether an axon is degenerated or not, and there are no variations of what type of fragments are excluded from degenerative data. Another advantage is that the researchers used an automated microscope stage to get pictures in consistent areas across the DRG sample, along with the assurance of carefulness and consistency when it comes to handling the cells. The authors suggest that this program may work for other models of neurodegeneration as well– such as those brought on by oxidative stress (Johnstone et al. 2018).

Another example of a team investigating changes of total neurite outgrowth length in relation to neurite degeneration is the work of a research group that made use of stereology to examine degeneration. The experimenters began by performing an intercranial injection of 6-OHDA into the nigrostriatal pathway of a rat brain. In order to count axonal projections in a 3D sample (tissue), the Spaceballs stereological probe was utilized. This instrument estimated length in a 3D region for normal and dystrophic axons. Dystrophic axons may be fragmented, twisted or present with blebbing. This tool worked by creating a 3D hemi-sphere embedded within the tissue slice being examined. Each projection that intersected the exterior bounds of the sphere was counted to create an estimate of the total length per region examined. The results showed that the treated brain areas showed a dying back pattern of neurodegeneration in response to 6-OHDA, even areas of the brain not directly related to the injection site showed degeneration since

the axons are the first things to become damaged. The researchers also noted that dystrophic axons generally had larger diameters than healthy ones. This was an example that related to an *in vivo* study to give more information on types of methods used to quantify neurite degeneration. Our research is an *in vitro* model that makes use of a degeneration index.

Prior research also indicates that measuring a degeneration index (D.I.) may be helpful when quantifying neurite degeneration. This is the process where total neurite area of a binarized microscopic image is measured in pixels in the FIJI software and then that number acts as the denominator in an equation. The numerator of the equation is the total pixel area occupied by fragmented neurites. To measure neurite area the particle analyzer function in FIJI is used to detect particles/fragments of a certain pixel size and circularity. Prior to any measurement of neurite area, the cell bodies present in the micrograph are manually selected and removed via use of the eraser tool in FIJI. The D.I. is calculated as the ratio of fragmented neurite area over total neurite area. This gives a representative number to symbolize the degree of fragmentation a particular treatment condition may have on neurites (Sasaki et al. 2009). Since this is a ratio, a numerically smaller number represents a healthy culture, and a larger number represents a degenerated culture. This is a common method for quantifying neurite degeneration via performance of a D.I. calculation. While this method has been used by different research groups, it is normally a manual method that may be prone to user error and investigator bias (Sasaki et al. 2009). To help alleviate some error that occurs with these techniques, we have optimized the method to increase its accuracy, efficiency, and user-friendliness.

Our Research

Our experiments have tested the implementation of several modifications designed to increase efficiency, accuracy, and accessibility, when compared to traditional methods for performing degeneration index calculations. These adjustments include using the background correction function of the microscope during the image capture process. Once the images have been obtained and are brought into the FIJI software, brightness and contrast of the image may be adjusted and enhanced in order for more accurate representation of neurites. FIJI is unique in that investigators may create their own programs to accomplish tasks not originally programmed within the software. These programs may be uploaded and used, and they are referred to as plugins. One such plugin removes particles of certain size and circularity that investigators may want to exclude from their data. When it comes to measuring the fragmented neurites, the pixel particle size detection range makes a difference in the output D.I. results. We also have modified selection criteria for fragmented neurites. Another change we implemented is use of fluorescent micrograph images as opposed to phase contrast images. Our research makes use of immunostaining for the β-III tubulin protein to obtain fluorescent signal to be visualized via fluorescent microscopy. This is a protein also referred to as TUJ-1 that comprises the microtubule network of the cytoskeleton. Microtubules are hollow tubes that play a role in processes like mitosis and motility, and they are made up of two subunits: alpha and beta tubulins. Depending on a cell's need, microtubules can rapidly grow/shrink via polymerization processes. Specifically, β-III tubulin is found in neurons and it has functions in neurogenesis and axonal maintenance (Jouhilahti et al. 2008). The largest and most helpful enhancement tested involves the automation of the entire process

to quickly and efficiently obtain accurate D.I. scores so that neurite degeneration may be quantified. For this process to work, there was also immunostaining using 4',6'-diamidino-2-phenylindole (DAPI). This is a fluorescent stain that selectively binds to the adenine-thymine-rich regions of DNA allowing for visualization of the nuclei. In our automated method binarized DAPI images are subtracted from binarized neurite images to automate the process of cell body removal. Since neurite degeneration is a key, early-stage event associated with PD, this optimized and automated method may be used to gain novel insights into molecular interactions underlying PD progression.

Experimental Procedures

Coating Slides

Eight well chamber slides from the brand SPL Life Sciences were used in our experiments. The slides were initially coated with 200 µg/mL poly-L-ornithine (Sigma) for at least twenty-four hours and then were washed with sterile water. The slides were then coated with 2 µg/mL fibronectin (Sigma) for three hours while incubated at 37℃. After incubation, the slides were once more washed with sterile water and then were covered with 100 ng/mL poly-D-lysine (Sigma), and 10 µg/mL laminin (Corning, Corning, NY) for another twenty-four-hour period. Once this time had elapsed, the slides were washed for one final time and were left out to air-dry and then were stored at 4℃ until further use.

Cell Culture

To emulate the dopaminergic cells that are destroyed in Parkinson's Disease, in our experiments we used Lund human mesencephalic (LUHMES) cells. The cells were

plated at a cell density of 85,000 cells/well to ensure enough separation between neurite tracts yet still consisting of a healthy culture. Cells were incubated in growth medium consisting of DMEM/F12 (Gibco, Waltham, MA) supplemented with 2 mM glutamine (VWR, Radnor, PA), 1% (v/v) N-2 supplement (Gibco), and 40 ng/mL basic fibroblast growth factor (R&D Systems, Minneapolis, MN). Once the cells had proliferated enough times and were of a confluency fit for treatment, they were differentiated into post-mitotic neurons by replacing their growth media with a media which also included 1 µg/mL tetracycline (Sigma), 1 mM N6,2′-O-Dibutyryladenosine 3′,5′-cyclic monophosphate (db-cAMP) (Enzo Life Sciences, Farmingdale, NY), and 2 ng/mL glial cell line-derived neurotrophic factor (GDNF)(R&D Systems). These components were added into a media that included DMEM/F12 + N2 supplement. The basic fibroblast growth factor was not included in this mixture, as to not promote further cell division. Cells received a half-volume media change every other day prior to treatment.

Cell Treatments and Fixation

Once cells reached their fifth day of differentiation, they were either treated with varying concentrations of 6-hydroxydopamine (6-OHDA) (Sigma), 4-hydroxynonenal (HNE) (Cayman Chemical, Ann Arbor, MI), or vehicle solution. 6-OHDA was prepared in cold phosphate-buffered saline (PBS) containing 0.02% ascorbic acid, and HNE was dissolved in chilled absolute ethanol. All aliquots of 6-OHDA and HNE were stored at -80^{o} C under inert gas and protected from light. To assess the effects of c-Jun N-terminal Kinase (JNK) on neurite degeneration some experiments involved pretreatment with the JNK inhibitor SP600125 (Sigma-Aldrich). This was to show that our technique worked with changing variables. All inhibitors were prepared in DMSO and stored under inert

gas in frozen aliquots that were protected from light. The cells were treated for twenty-four hours and then were fixed. The fixation process involves exposing the treated cells to 4% paraformaldehyde (PFA) for a twenty-five-minute period and then they were placed in sterile PBS.

Immunostaining

Once cells were fixed, they were immunostained to visualize ßIII-tubulin protein and the nucleus of the cells. After fixation, the cells were permeabilized using 0.1% Triton™ X-100 (Sigma-Aldrich) in PBS. The cells were then blocked for one hour in PBS containing 10% normal goat serum and 0.1% Triton™ X-100. The cells were then incubated at 4℃ overnight while exposed to the primary antibody for ßIII-tubulin (Covance, Princeton, NJ; 1:1000). The following day the cells were washed twice using and 0.1% Triton™ X-100 and twice with sterile PBS and then were placed in secondary antibodies coupled to the Alexa Fluor 488 (Thermo Fisher Scientific; 1:1000) fluorophore. After 90 minutes at room temperature elapsed, the cells were then washed again twice using and 0.1% Triton™ X-100 and twice with sterile PBS and then 5 µg/mL 4’,6’-diamidino-2-phenylindole (DAPI) in PBS was applied for 5 minutes at room temperature. After the cells were incubated in DAPI the cells received a final wash, twice using and 0.1% Triton™ X-100 and twice with sterile PBS and the slides were cover slipped using Fluoromount-G® mounting medium (Southern Biotech, Birmingham, AL). All slides rested in a dark and dry place for at least 24 hours before any type of microscopy imaging took place.

Image Capture

For capturing images of the treated cells, the NIS Elements Acquisition software was used in conjunction with a Nikon inverted microscope. Kohler illumination was performed prior to each image capture session. Cells were visualized using both phase contrast (PC) and fluorescent microscopy. For phase contrast microscopy images were captured at a 20x magnification and with a gain of 1.00x and a 21 second exposure time. The plain filter turret was used for PC images. For all images, the correction collar on the objective was set to 0.17 and the light intensity dial was set to the beginning of the seventh highest light intensity notch. Prior to image capture of the cells there was a background image taken and background correction was applied within the software for each PC image captured. For each well of the slide there were five representative images taken. Preferred areas to image were areas where the neurite tracts were clearly defined, and cells were not too confluent or sparse. The images were saved as TIFF and ND2 files. While keeping the location frame the exact same for each image, fluorescent images were also taken. For these images specifically the green filter turret was used to view the TUJI staining and the exposure time was 1 second. The background correction function was not used for fluorescent images. The spinning disk filter was adjusted to shine the blue LED light onto the sample of cells. Normal exposure times for fluorescent images ranged from 900 ms-2 s. The gain was set at 1.20x. After the fluorescent images were captured the LED light source was removed from the sample to prevent photo-bleaching the cells.

Once PC and fluorescent images to visualize β-III tubulin were taken for each representative area within the well, DAPI images were also taken for those same areas. To do this the blue filter turret was used and the exposure time was 125 milliseconds with

a gain of 2.80x. The background correction function was not used for DAPI images, and the ultraviolet disk was used. The same care was taken to avoid photo-bleaching for DAPI images. Once the PC, fluorescent, and DAPI images were taken for each area of the well they were saved as both TIFF and ND2 files and were then ready to be processed and quantified. Then these files were sorted into PC, fluorescent, and DAPI folders on the computer for organizational purposes.

Traditional DI calculation

FIJI software was used to analyze the images. Traditional DI calculations were performed by opening the images as TIFF files with FIJI and then all five images from each area of a well were viewed and manipulated at the same time by putting the images into a stack. For PC images the background was set to white and the foreground color was set to black. The images were then binarized and the cell bodies were removed using a tablet, stylus, and the eraser tool function in FIJI. Particle analyzer function was used. To measure total neurite area the measure setting was used, and the number was recorded. To measure neurite fragments the analyze function was used measuring size from 20-10,000-pixels and the circularity settings were 0.20-1.00. This number was recorded and then neurite fragment area was divided by the total neurite area to obtain a D.I. This process was repeated for each treatment condition well.

Optimized DI calculation

The traditional method had issues, and so within our research we made use of an optimized method to quantify neurite degeneration. After traditional image capture and putting the TIFF files into FIJI the images then had their contrast and brightness levels

adjusted such that the lookup table ranged from 90-205. The images were then binarized and the cell bodies were removed using a tablet, stylus, and the eraser tool function in FIJI. Once the cell bodies were removed from the images, the particle remover plugin was used to remove small, non-neurite debris and artifacts from the image. This was used with the settings of a size of 0-9.0 pixels and a circularity of 0.20-1.00 to remove these specific particles. Once the particles were removed to a white background, then the measure and particle analyzer functions were used. To measure total neurite area the measure setting was used, and the number was recorded. To measure neurite fragments the analyze function was used measuring size from 10-10,000-pixels and the circularity settings were 0.20-1.00. This number was recorded and then neurite fragment area was divided by the total neurite area to obtain a DI. This process was repeated for each treatment condition well.

Macro Development

An important feature of the automation process was the development of a macro to incorporate all the modifications for enhancement. Depending on if the starting image is a PC or fluorescent image the macro maybe different. One additional folder was made on the computer for each well to organize output images. For PC images the major steps performed by macro are as follows: open neurite image> convert to an 8-bit image> adjust brightness and contrast so that the grayscale range is 90-205> adjust the colors so that the foreground is black and the background is white> binarize image> use of particle remover plugin to remove particles with a size between 0-9.0 pixels and a circularity of 0.00-1.00 pixels> open DAPI image> convert to an 8-bit image> adjust brightness and contrast so that the grayscale range is 0-195> binarize image> use of particle remover

plugin with a size setting of 0-9.0 pixels and a circularity of 0.00-1.00 pixels> dilate ten times> erode four times> subtraction of DAPI image from the neurite image> take measurement of new area of image> particle analysis using a 10-10,000-pixel size and a 0.20-1.00 circularity>save results. The results for total neurite area and fragmented particle area are saved and exported to an excel file for viewing and calculation of the D.I.

Fluorescent images were processed in a similar fashion, with the exception that when the brightness and contrast was adjusted initially for the neurite image, the lookup table range was from 0-195. After the automated method was applied, D.I. values were calculated for each well's treatment condition.

Results and Figures

In the present research we found a way to better enhance accuracy and efficiency of the quantification of neurite degeneration. From qualitative data, we observed differences between the traditional and enhanced method. The following figure depicts a schematic of the traditional method used to calculate a D.I. Within this process image capture using PC microscopy occurs as shown in panel 1A. Images are then opened in FIJI and then binarized, as shown in panel 1B. Panel 1C presents the result of manual cell body removal. Total neurite area is measured and then particles with a pixel size of 20-10,000-pixels are detected in panel 1D and then a D.I. is calculated in panel 1E.

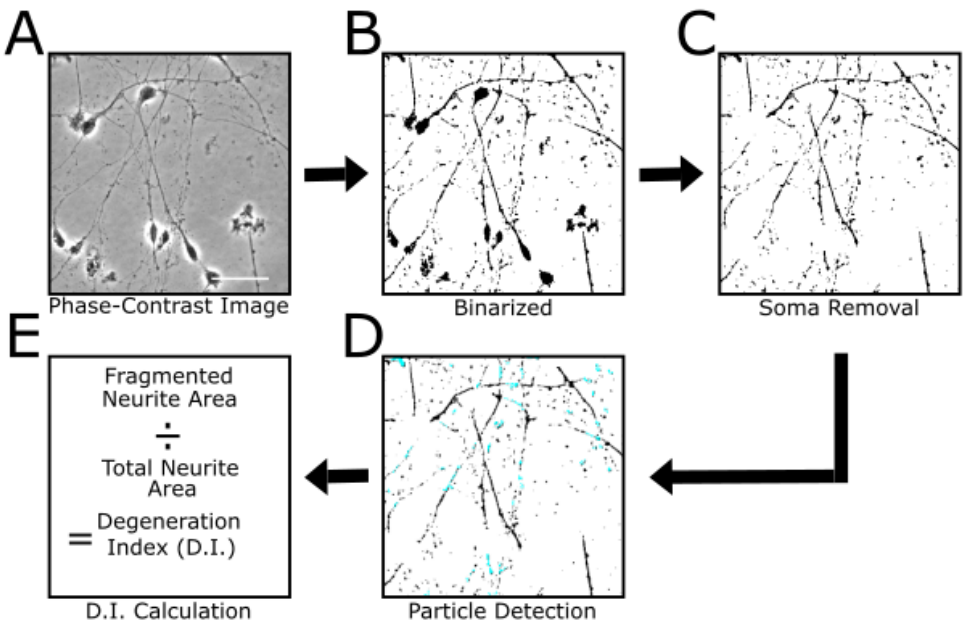

Figure 1. **Traditional method for quantifying neurite degeneration with a degeneration index (D.I.)**. **A**; a phase contrast image of the treated LUHMES cells **B**; binarized version of the

phase-contrast image once the image has been put into FIJI software **C**; soma/cell body removal via use of the eraser or freehand selection tool in FIJI **D**; particle detection of fragments that have a size of 20-10,000-pixels and a circularity of 0.20-1.00 **E**; Calculation of the degeneration index (D.I.) that represents the ratio of fragmented neurite area over total neurite area. The scale bar indicates 100 µm.

Additional steps in the image acquisition process were added so that issues with background shading once an image was binarized could be alleviated. The image set in Figure 2. shows the qualitative data for using background correction settings within the Nikon microscope acquisition program. In this figure we see visually a phase contrast image in panel 2A that was captured without background correction being applied. Once

binarized, shown in 2B, the image presents with a lot of background shading that will influence the total neurite area. This is in contrast to the PC image that does have background correction applied in 2C. Once this image has been binarized, shown in 2D, it appears to more accurately depict the neurites without any shading that will affect the D.I. calculation.

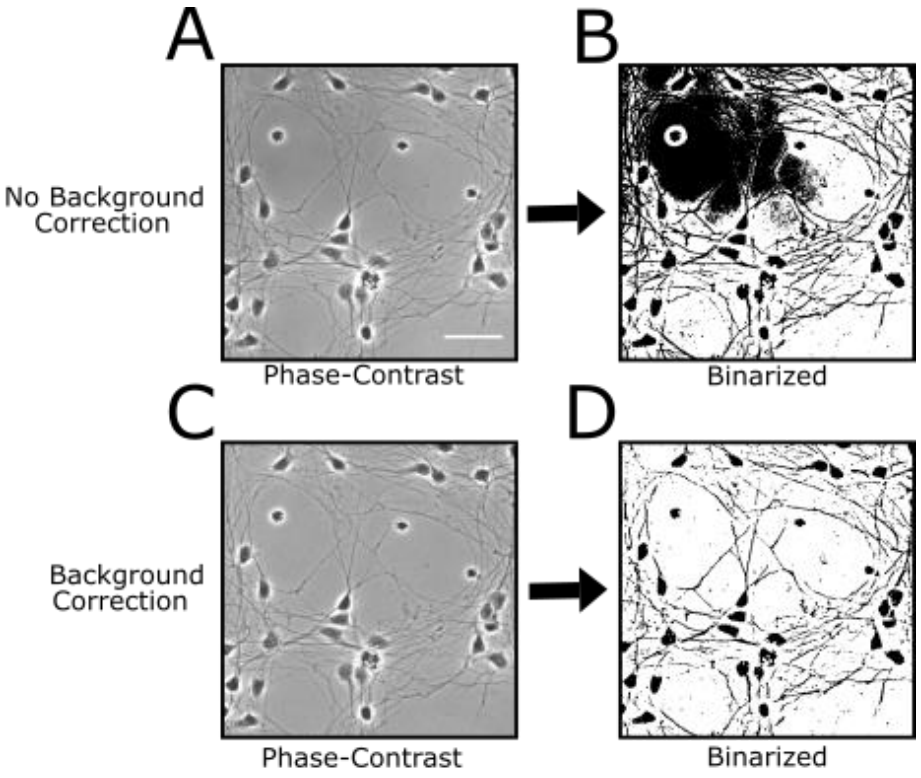

Figure 2. **Use of the background correction function during image acquisition**. **A**; indicates an original phase contrast (PC) image that was captured without background correction **B**; the binarized version of the PC that presents with background shading **C**; indicates an original PC image that was captured with background correction **D**; the binarized version of the PC image that had background correction applied. The scale bar indicates 100 µm.

Once images were opened in the FIJI software there were additional modifications made that related to contrast and brightness. The effect of these adjustments are shown in Figure 3. These levels were adjusted so that neuron structure better stood out from the background. Poor contrast was an issue that detrimentally affected the accuracy of binarized PC images; once the images with poor contrast were binarized (3A and 3C), healthy neurites presented as being fragmented in a sort of artificial fragmentation. Once the brightness and contrast levels were optimized for a PC image, the binarized version had a reduction in artificial fragmentation (3B and 3D).

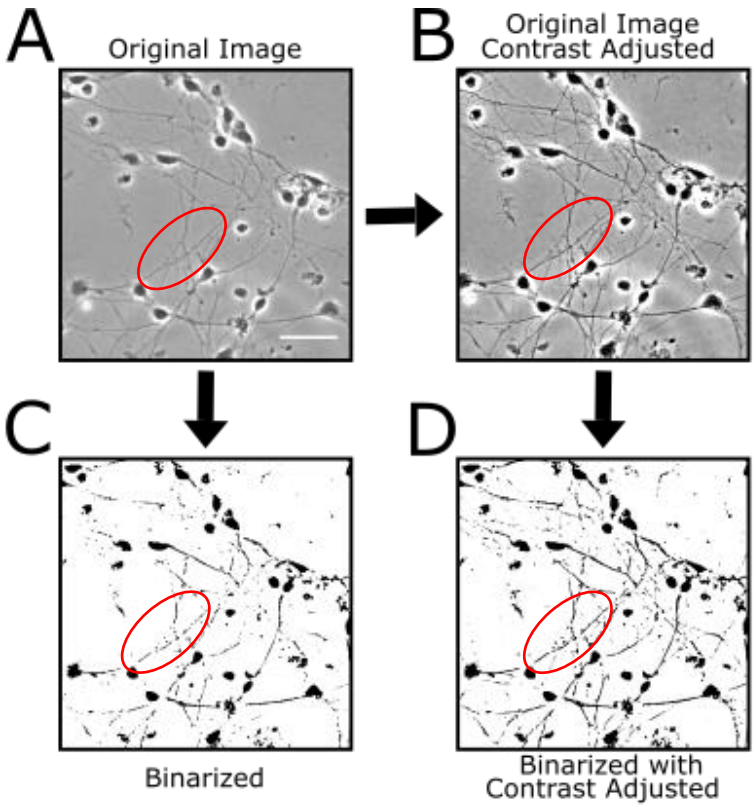

Figure 3. **Brightness and contrast adjusted images**. **A**; indicates and original phase contrast image, as shown, the neurite highlighted within the red oval has low contrast **B**; the manipulated PC image that has brightness and contrast enhancements applied in FIJI,

making the neurite more noticable **C**; the binarized version of the original PC image that presents with artificial fragmentation of the neurite **D**; the binarized version of the manipulated PC image that more accurately resembles the healthy neurite from images A and B. The scale bar indicates 100 µm.

When it comes to measuring area of the neurites, another function we implemented for establishing our enhanced method made use of the particle remover plugin in FIJI. This plugin visually and qualitatively removes a lot of the background shading that may occur in an image once it is binarized. Such artifacts can result from cellular debris or dust, or from not using background correction during image acquisition. In this image set shown in Figure 4 we can see the difference between using the plugin set to remove particles that are between 0-9.0 pixels (4B) and not using this function (4C). Once binarized, artificacts show up that are unrelated to neurite fragments. Additional experimental data that is from the treatments of cells with the drugs 6-OHDA and HNE shows that use of the particle remover plugin corresponds to higher D.I.s being calculated among nearly every treatment condition, since the meausured total neurite area will be decreased. In this data shown in 4D and 4E, the dark bars indicate use of the traditional method and the gray bars indicate D.I.s calculated with use of the particle remover function. It seems that treatment with HNE causes severe degeneration between vehicle and experimental conditions, as shown in 4E. It also appears that treatment with 6-OHDA has a more dose-dependent effect relating to drug concentration on degeneration, as shown in 4D.

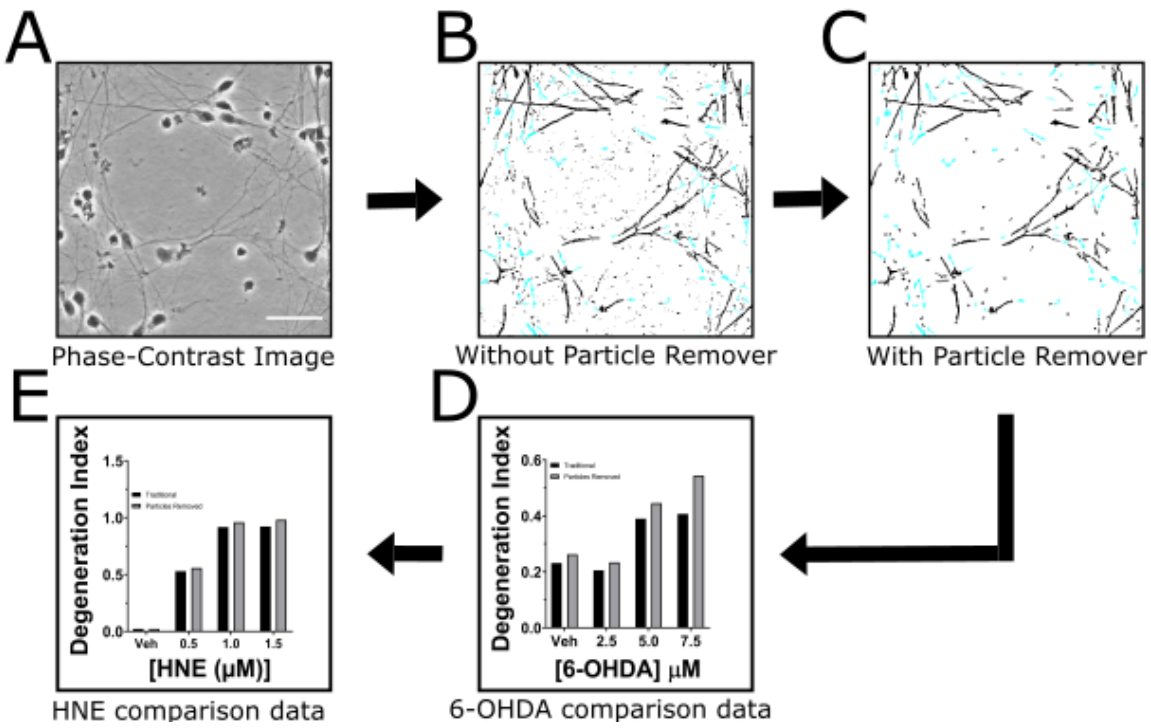

Figure 4. **Use of the particle remover plugin's effect on D.I. A**; represents an original PC image **B**; binarized PC image with soma removal without the use of the particle remover function, seen with a moderate amount of background artifacts across the image **C**; binarized PC image with soma removal with the use of the particle remover function, less artifacts show up and a cleaner image is presented **D**; D.I. data from a 6-OHDA experiment to assess dose effects on neurite degeneration (n=1). This data shows the method that makes use of the particle remover (gray bars) results in higher D.I.s quantitatively than when in comparison to the traditional method (black bars) **E**; D.I. data from an HNE experiment to assess dose effects on neurite degeneration (n=1). This shows the method that makes use of the particle remover (gray bars) results in higher D.I.s quantitatively than when in comparison to the traditional method (black bars). The scale bar indicates 100 µm.

D.I. calculations are influenced by particle detection size. In the enhanced method another optimization we made narrowed selection criteria for fragmented neurites. These fragments are highlighted and detected if they are between a 10-10,000-pixel size. This is in comparison to the traditional method that does not include particle removal and only measures neurite fragments that are between a 20-10,000-pixel size. In Figure 5 the accuracy differences between using a 10-10,000 (5D) and a 20-10,000 (5C) pixel detection range is shown. The latter image in 5C presents with more artifact and background shading that may affect total neurite area, and there are neurites that are not being detected.

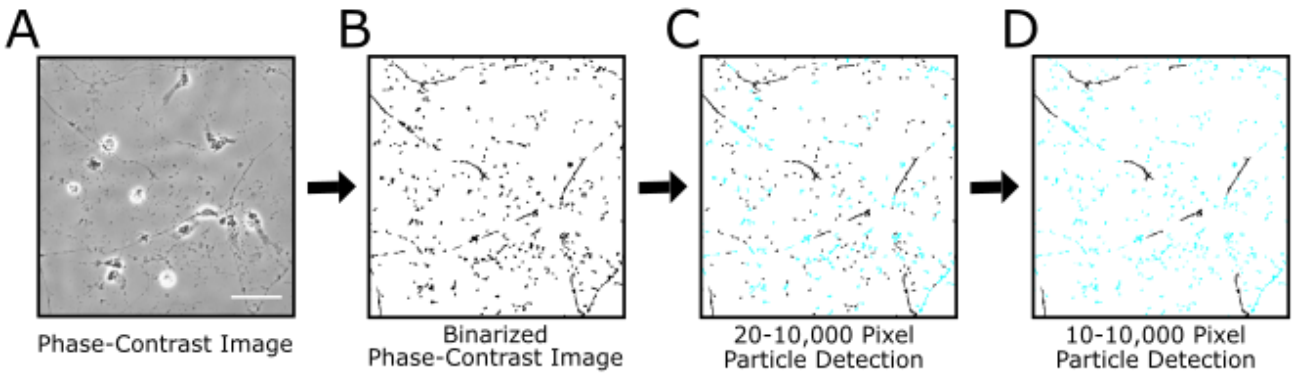

Figure 5. **Difference between the traditional and enhanced method when it comes to pixel particle detection size**. **A**; original PC image of a degenerated culture **B**; binarized PC image with soma removal **C**; binarized PC image with soma removal that has particles of a 20-10,000- pixel size being detected, representative of the traditional method **D**; binarized PC image with soma removal that has particles of a 10-10,000-pixel size being detected, representative of the enhanced method. The scale bar indicates 100 µm.

The traditional method is set up so that during image capture phase-contrast microscopy is performed. To qualitatively and quantitatively show that fluorescent images provide a more accurate starting image we stained and used fluorescent images to obtain D.I. calculations. The following figure shows the qualitative difference between using PC and fluorescent images to begin with. The difference becomes apparent once binarized. The original PC image binarizes to include background shading and artifacts. The original fluorescent binarized image is much clearer with less background noise and non-neurite artifacts. The field of view is of a vehicle condition well so the neurons should be healthy and not present with artifacts/ fragmentation. This image set also includes data from a 6-OHDA experiment to assess dose effects on neurite degeneration (n=1). The data indicates that use of fluorescent microscopy enhances the sensitivity with which D.I. analyses detect neurite degeneration. D.I. The black bars in panel 6E indicate the use of original PC images and the gray bars in panel 6E indicate the use of original fluorescent images. The enhanced method presents a more dose dependent effect on degeneration when measured using fluorescent images, as shown in 6E.

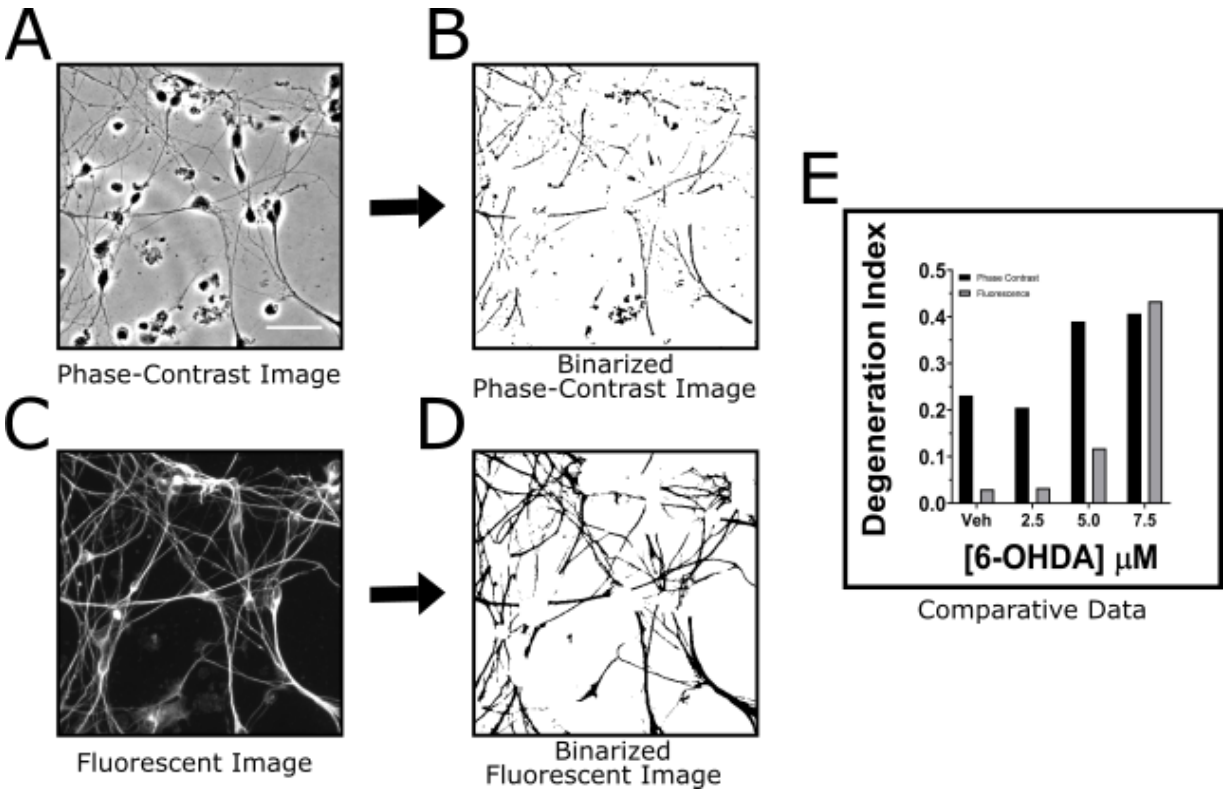

Figure 6. **Use of phase-contrast vs fluorescent images**. **A**; PC image that has had brightness and contrast enhancements **B**; binarized PC image that has had brightness and contrast enhancements with soma removal **C**; fluorescent image of staining for the β-III tubulin protein **D**; binarized fluorescent image with soma removal. **E**; D.I. data from a 6-OHDA dose response treatment to assess dose effects on neurite degeneration (n=1) that shows the difference in D.I. for the method that uses original PC images (black bars) and the method that uses original fluorescent images (gray bars). The scale bar indicates 100 μm.

As this research developed, a leading motivation for our work began to shift towards focusing on creating an automated method for the whole process. The automation of the enhanced method makes the whole process more efficient since accurate results may be compiled within a fraction of the time of the traditional method. The schematic in Figure

7 depicts the automated method and how it works. To automate the method a macro in FIJI has been developed. Within this method, a fluorescent image that has had brightness and contrast enhancements has been binarized with unwanted particles removed. This image serves as “neurite staining” image, as shown in panel 7A. A secondary fluorescent image of DAPI nuclear staining is opened. This image has also had brightness and contrast enhancements. It has also been binarized with unwanted particles removed, and it serves as the “DAPI image”, shown in panel 7B. The outside perimeter of the DAPI staining is then expanded ten times using the dilate function and then slightly made smaller using the erode function four times. This step is to allow for the nuclear stain to emulate a cell body more closely, shown in 7C. The dilated and eroded DAPI image is then subtracted from the neurite image to obtain a picture of the neurites without cell bodies (7D). Total and fragmented neurite areas are measured and recorded so the D.I.s may be calculated. In panels 7E and 7F additional 6-OHDA treatment data is shown from PC (n=1) and fluorescent 6-OHDA (n=1) experiments, to assess dose effects on neurite degeneration. For both PC and fluorescent experiments, the automated and the manual method show similar D.I. numerical values. The dark bars indicate the manual method, and the gray bars indicate the automated method, both shown in 7E and 7F. Both experiments show a dose-dependent increase in D.I. values for both of the methods.

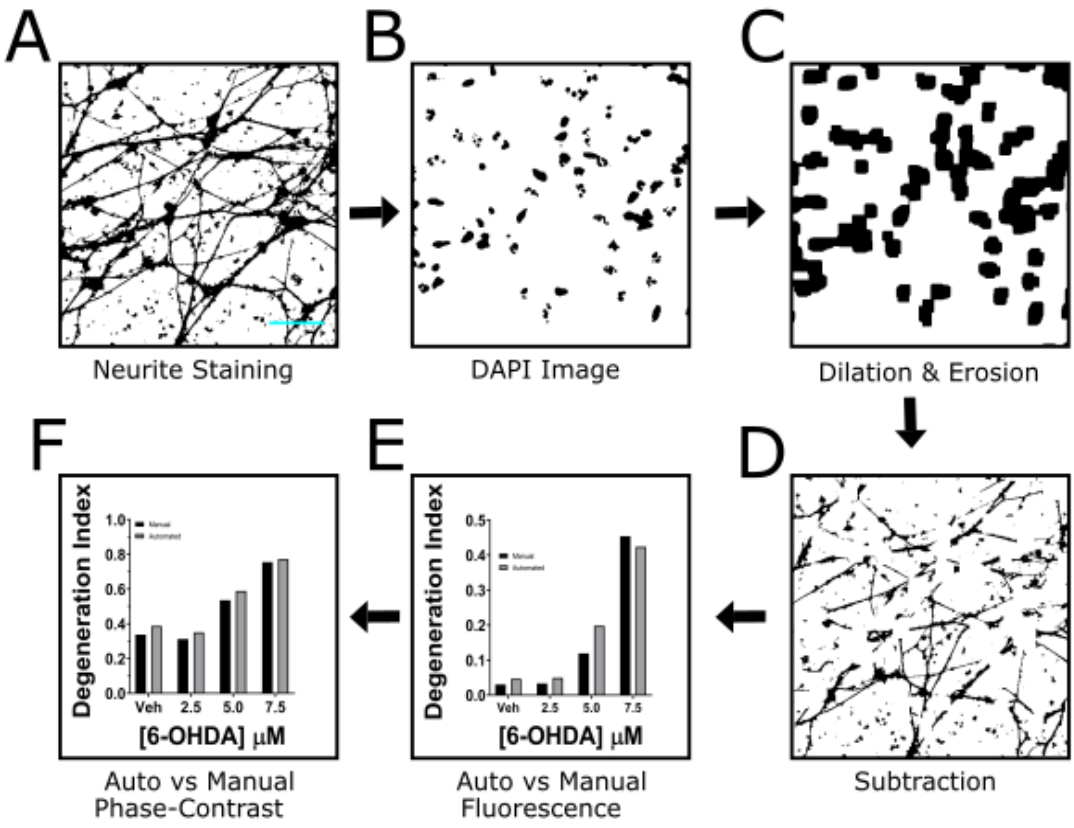

Figure 7. **Automated vs manual methods for quantification of neurite degeneration**. **A**; Binarized fluorescent image that has had brightness and contrast enhancements with particles removed **B**; binarized DAPI image that has had brightness and contrast enhancements with particles removed **C**; dilation and erosion processing of DAPI image **D**; represents the resulting image obtained after the dilated and eroded DAPI image has been subtracted from the neurite staining image **E**; Fluorescent D.I. data from 6-OHDA experiment to assess dose effects on neurite degeneration (n=1) that shows the difference in D.I. for the manual method (black bars) and the automated method (gray bars) **F**; PC D.I. data from 6-OHDA experiment to assess dose effects on neurite degeneration (n=1) that shows the difference in D.I. for the manual method (black bars) and the automated method (gray bars).

Automation of the process greatly increases efficiency. Time estimate data (n=1) for both automated and manual methods was performed by using a stopwatch to record the time it took to make any necessary modifications and to calculate the D.I. for all the image sets within an experiment. Preliminary time data shows that the automated process took a shorter amount of time. For the manual method, average processing time for a fluorescent image set was 3.1356 minutes/image. In comparison, the average automated method only took 0.448 min/image. For a whole dataset with up to 35 images the manual method took 1 hour 50 minutes and the automated method took 15.68 minutes to complete.

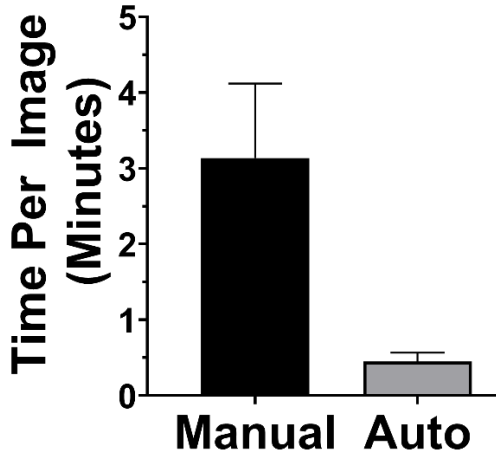

Figure 8. **Automated vs manual methods time estimate data.** The dark bar indicates the time required to perform the manual method on a fluorescent image set, registering with an average time of 3.1356 min/image for processing time. The time required to perform the automated method is indicated by the gray bar, registering with an average processing time of 0.448 min /image.

Finally, we sought to demonstrate use of our optimized method in an experiment assessing the effects of c-Jun N-terminal Kinase (JNK) on neurite degeneration. To do this, we treated LUHMES cells with vehicle, 6-OHDA and SP600125+6-OHDA treatment conditions and compared D.I.s. Our results indicated that our optimized method allowed us to determine that JNK activation is required for neurite degeneration induced by oxidative stress. The data shown in Figure 9 presents the numerical D.I. data for

vehicle, 6-OHDA and SP600125+6-OHDA treatment conditions. The SP600125 was used in order to inhibit JNK activation, which lead to a decrease in D.I., corresponding to a decrease in degeneration. There is a significant difference between the D.I.s calculated for the vehicle and 6-OHDA treatment condition. However, is no significant difference between vehicle and SP600125+6-OHDA conditions, which indicates the inhibitor properly worked to inhibit JNK activation.

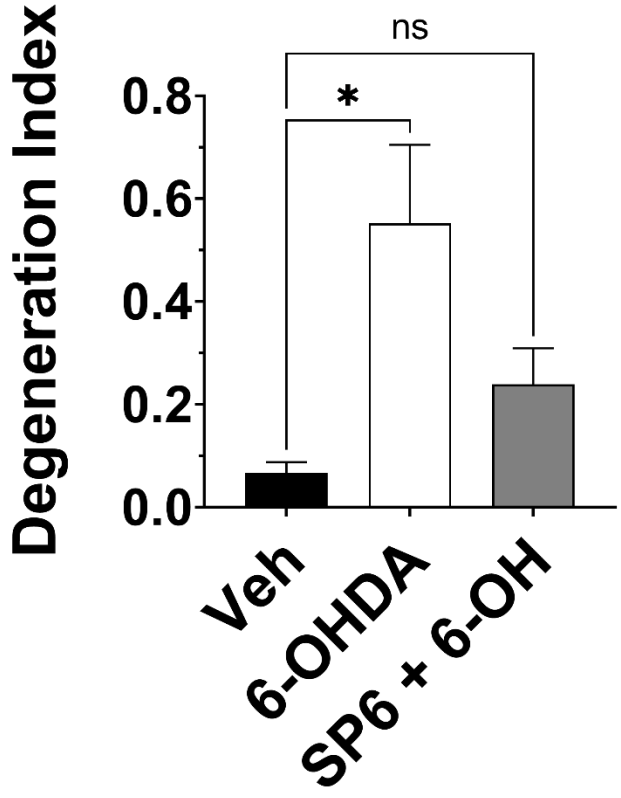

Figure 9. **Degeneration data for an SP600125 experiment**. **Veh** indicates treatment of cell culture with control conditions, these cells are only treated with what SP600125 and 6-OHDA are dissolved in, which was DMSO and PBS with 0.02% ascorbic acid. **6-OHDA** indicates treatment with the drug 6-OHDA, triggering the activation of JNK (a protein activated in the stress signaling pathway). This was a dose dependent experiment spanning 24-hours, with a 7.5 µM 6-OHDA treatment condition. **SP6+ 6-OH** indicates a one hour pretreatment with the JNK inhibitor SP600125 prior to 24-hour treatment with 7.5 µM 6-OHDA (n=4).

These results reveal that the optimized method can accurately be used across all treatment conditions.

Discussion

Measuring neurite degeneration is an important avenue of research. Advances in this area of research may facilitate development of new therapies. As previously discussed, there are issues with existing methods for analyzing neurite degeneration. Once we began to research this topic, we applied a method previously described (Sasaki et al. 2009) and found several issues with it. In relation to background correction, the previously described traditional method to quantify degeneration using D.I. scores did not have any information relating to background correction or lighting at the time of image capture. This was an apparent issue once we began to apply the technique since once an image was binarized, if it did not have appropriate lighting with background correction applied, then the image had severe background shading that drastically altered the appearance of the image. Total neurite area that was measured was also affected, as seen in Figure 2. Our enhanced method featured use of background correction and optimized microscope lighting such that the average grayscale level was at 165, resulting in a clearer and seemingly more accurate binarized image.

Other issues with the traditional method also relate to exposure times and gain settings of the microscope. Previously published methods had little information of these specifics, yet they still made a difference once an image was binarized. Our team found it to be beneficial to capture images at a 20x magnification for all image types. For phase contrast images gain was set at 1.00x with a 21 second exposure time. For fluorescent images visualizing TUJ-1, gain was set at 1.20x with an exposure that ranged from 900

ms to 2 seconds. DAPI images were captured with a 2.80x gain and a 125 ms exposure time for best results. These settings are specifically for a Nikon inverted microscope.

The act of performing brightness and contrast enhancements is also an important step to take to get an accurate neurite fragment area measurement. If this step is not properly performed there may be artificial fragmentation that occurs, as depicted in Figure 3. The same reasoning applies for use of the particle remover plugin within FIJI. Use of this function affects the total neurite area that is recorded, as shown in Figure 4. In the enhanced method the smallest neurite fragments that are measured are 10.0 pixels, and so it is necessary to remove anything smaller than that to get an accurate measurement. Another way the enhanced method has improved upon the traditional method is also seen qualitatively in difference in particle detection size, shown in Figure 5. Detection of particles between 20-10,000-pixels does not identify all the fragments that show up within the image, and so it is also necessary to drop the threshold of detection to measure between 10-10,000-pixel particles.

When examining Figure 6, there is more qualitive data that supports the use of original fluorescent images for the enhanced method. Once binarized the fluorescent images present with much less background noise when compared to phase contrast images. These findings are further supported by data from another group who also used β-III tubulin and fluorescent images to quantify neurite degeneration. In their studies cells were exposed to *m*-Dinitrobenzene (*m*-DNB), a selected model neurotoxicant, and then immunostained and visualized with fluorescent microscopy. They also increased contrast by using the Enhance Local Contrast (CLAHE) plugin within FIJI to outline cell morphology more precisely. Their images were then binarized in order to threshold to

create a contour of the area of the cell and the count particles plugin was used to identify neurite fragmentation. Based on visual observations of several images of neurites, particles below 2.5 μm were considered to be either debris or background artifacts. Then they compared time trial data to see the effect the *m*-DNB had on neurite degeneration. As expected, the neurites exposed to higher concentrations of *m*-DNB for longer periods of time had higher amounts of degeneration (Dixon and Philbert 2016).

Another study relating to microtubules gives support for using β-III tubulin to showcase neurite degeneration. Reduction in neurite length, number of neurite branches and synaptic terminals, seen in PD patients, has been linked to increased microtubule depolymerization in the absence of functional Parkin. This is an important enzyme involved in ubiquitination- the process whereby molecules are covalently labelled with ubiquitin (Ub) and get labeled for destruction via proteasomes or lysosomes (Dubey et al. 2015). This supports the idea that β-III tubulin may have the same pattern of degradation as neurites.

The enhanced method that we have created also alleviates the issue of subjectivity that prior methods have. For example, the research team previously discussed, led by Engelmann, counted axons by use of a blinded examiner, however depending on the examiner, the results may have been subjective (Engelmann et al. 2020). In the manual method of obtaining a D.I., there is the step of using the eraser tool within FIJI to erase cell bodies and artifacts unrelated to neurites. This step may lead to inaccuracies due to subjectivity of what an investigator deems to be a cell body or not. Sometimes it may be difficult to tell if a neurite is connected to a cell body or a blebbed section, so depending on the individual doing the manual cell body subtraction, there may be differing D.I.

values produced for the same image. Subjectivity may also be introduced depending on what tool is used for the cell body subtraction. The free hand selection or the eraser tool may be used to eliminate the soma, however depending on which one is used, there also may be varying results. Other methods of quantifying neurite degeneration that may be associated with subjectivity include visually scoring neurite fragmentation on a scale of 0-1.0. This is much like giving a sample a D.I. score but instead of using mathematical measurement of areas, the investigator views the image and gives it a representative score. An advantage of our enhanced method is that it automates the cell body subtraction process and uses DAPI staining to identify nuclei uniformly and therefore cell bodies more objectively. It also leaves no room for user error or subjectivity since it is automated, containing programmed steps and use of a formula to create a score to represent fragmentation.

Another issue that relates to the manual method involves timing and efficiency. Cell body subtraction is subjective, but it is also very time consuming. On average for a fluorescent image set the manual method took 3.1356 min/image. This corresponded to a 1 hour and 50-minute complete processing time to obtain D.I. calculations for a whole data set. This is in comparison to the automated method that only took on average 0.448 min/image. This corresponded to a 15.68 min complete processing time for a whole data set, that included 35 images. The use of the macro within FIJI saves time and increases efficiency, since data sets can have up to 120 images and use of the macro allows simultaneous application of many modifications to whole image sets. Even before developing the automated method there were modifications made to try to save time when performing cell body subtraction. Investigators first began the process using a

computer mouse pad to select and circle areas deemed to be a cell body so that they could be deleted from the image. Use of a computer mouse helped to slightly quicken the process due to easier and more fluid wrist movements. However, it still was a lengthy process. Another adjustment made was using a touch screen tablet and a stylus along with the eraser tool to easily touch and delete cell body selections. Though this action made a pronounced difference in the time it took to remove cell bodies, it still took a drastically longer time than it took making use of the automated method.

In addition to being efficient the enhanced automated method is more user-friendly. The traditional method presented with issues that needed to be fixed in order to obtain accurate D.I. data. To correct these issues, adjustments were made using brightness and contrast settings, along with use of the particle remover function. Our method makes use of a macro which reduces the number of steps needed when compared to the traditional method. Our method also provides novice learners the information they need so they do not have to be experienced with FIJI in order to obtain accurate D.I. data, further simplifying the method.

Other groups in the past have used differences in overall neurite length as a way to quantify degeneration. For example, a research team compared neurons transfected with a control protein with neurons that had overexpression of the wildtype versions of α-synuclein. Their results indicated that neurite length significantly was reduced in the cells that contained α-synuclein (Furlong et al. 2020). This result is to be expected since one would assume if degeneration is occurring that there would be some type of fragmentation or shortening of the neurite. The problem with measuring neurite length to indicate degeneration presents itself when there is differing data that is published, which

seemingly makes the method itself seem unreliable. For example, another group that treated rat hippocampal neurons with 6-OHDA and SP600125 saw shortening of neurites of neurons that were treated with the SP600125 and elongation of cells that had JNK activation present (Eminel et al. 2008). JNK is a specific type of protein that plays a dual role in death signaling pathways and neurite outgrowth. This research team's effort is a good example of why measuring neurite outgrowth alone is not a reliable way to measure degeneration. Our SP600125+6-OHDA experiment to assess JNK's role on neurite degeneration data indicated higher degrees of fragmentation for cells that had been exposed to oxidative stress and lower D.I.s for the SP600125 pretreatment conditions. Our method seems to present more consistent results that align with other research that has reported on the damage that 6-OHDA may induce. The data presented in Figure 9 also validates use of the automated method within the context of an actual experiment. The D.I. values between the 6-OHDA and vehicle conditions were significantly different. The method that uses loss of neurite length to indicate degeneration may have issues due to the blebbing of neurites. A neurite may become blebbed but not have a significant change in overall length, or the neurite may become fragmented without a substantial change in length. Our method makes use of measuring neurite fragments so that it may be compared to total neurite area, so that issue does not apply with the enhanced method.

In conclusion, the method that we present is more accurate, efficient, and user-friendly than the traditional method of quantifying neurite degeneration making use of a degeneration index. Through modifications of the process relating to image capture and processing in FIJI, we have been able to develop an accurate, automated method. A future study that could help to further validate use of this new method could be to

compare the fluorescent β-III tubulin signal with whole cellular structure to further support the notion that β-III tubulin follows the same pattern of degradation as the neurites. Hopefully, this enhanced and automated method may be used to evaluate novel therapies relating to Parkinson's disease in the future.

Bibliography

Basu, S., & Dasgupta, P. S. (2000). Dopamine, a neurotransmitter, influences the immune system. *Journal of Neuroimmunology*, *102*(2), 113–124. doi: 10.1016/S0165-5728(99)00176-9

Bird, T. D. (1993). Alzheimer Disease Overview. In M. P. Adam, H. H. Ardinger, R. A. Pagon, S. E. Wallace, L. J. Bean, K. Stephens, & A. Amemiya (Eds.), *GeneReviews*®. Seattle (WA): University of Washington, Seattle. Retrieved from http://www.ncbi.nlm.nih.gov/books/NBK1161/

Bourdy, R., Sánchez-Catalán, M.-J., Kaufling, J., Balcita-Pedicino, J. J., Freund-Mercier, M.-J., Veinante, P., … Barrot, M. (2014). Control of the nigrostriatal dopamine neuron activity and motor function by the tail of the ventral tegmental area. *Neuropsychopharmacology: Official Publication of the American College of Neuropsychopharmacology*, *39*(12), 2788–2798. doi: 10.1038/npp.2014.129

Cenini, G., Lloret, A., & Cascella, R. (2019). Oxidative Stress in Neurodegenerative Diseases: From a Mitochondrial Point of View. *Oxidative Medicine and Cellular Longevity*, *2019*, 2105607. doi: 10.1155/2019/2105607

Creed, R. B., & Goldberg, M. S. (2018). New Developments in Genetic rat models of Parkinson's Disease. *Movement Disorders: Official Journal of the Movement Disorder Society*, *33*(5), 717–729. doi: 10.1002/mds.27296

Curtin, J. F., Donovan, M., & Cotter, T. G. (2002). Regulation and measurement of oxidative stress in apoptosis. *Journal of Immunological Methods*, *265*(1), 49–72. doi: 10.1016/S0022-1759(02)00070-4

Davis, M., Stroud, C., & Medicine, I. (2014). Neurodegeneration: Exploring commonalities across diseases: Workshop summary. In *Neurodegeneration: Exploring Commonalities Across Diseases: Workshop Summary* (p. 106). doi: 10.17226/18341

Dixon, A. R., & Philbert, M. A. (2015). Morphometric Assessment of Toxicant Induced Neuronal Degeneration in Full and Restricted Contact Co-cultures of Embryonic Cortical Rat Neurons and Astrocytes: Using m-Dinitrobezene as a Model Neurotoxicant. *Toxicology in Vitro : An International Journal Published in Association with BIBRA, 29*(3), 564–574. doi: 10.1016/j.tiv.2014.12.015

Dubey, J., Ratnakaran, N., & Koushika, S. P. (2015). Neurodegeneration and microtubule dynamics: Death by a thousand cuts. *Frontiers in Cellular Neuroscience*, *9*. doi: 10.3389/fncel.2015.00343

Eminel, S., Roemer, L., Waetzig, V., & Herdegen, T. (2008). C-Jun N-terminal kinases trigger both degeneration and neurite outgrowth in primary hippocampal and cortical neurons. *Journal of Neurochemistry*, *104*(4), 957–969. doi: https://doi.org/10.1111/j.1471-4159.2007.05101.x

Engele, J., & Franke, B. (1996). Effects of glial cell line-derived neurotrophic factor (GDNF) on dopaminergic neurons require concurrent activation of cAMP-dependent signaling pathways. *Cell and Tissue Research*, *286*(2), 235–240. doi: 10.1007/s004410050692

Engelmann, S., Ruewe, M., Geis, S., Taeger, C. D., Kehrer, M., Tamm, E. R., … Kehrer, A. (2020). Rapid and Precise Semi-Automatic Axon Quantification in Human Peripheral Nerves. *Scientific Reports*, *10*(1), 1935. doi: 10.1038/s41598-020-58917-4

Flynn, K. C. (2013). The cytoskeleton and neurite initiation. *Bioarchitecture, 3*(4), 86–109. doi: 10.4161/bioa.26259

Freed, C. R., Greene, P. E., Breeze, R. E., Tsai, W. Y., DuMouchel, W., Kao, R., … Fahn, S. (2001). Transplantation of embryonic dopamine neurons for severe Parkinson's disease. *The New England Journal of Medicine, 344*(10), 710–719. doi: 10.1056/NEJM200103083441002

Furlong, R. M., O'Keeffe, G. W., O'Neill, C., & Sullivan, A. M. (2020). Alterations in α-synuclein and PINK1 expression reduce neurite length and induce mitochondrial fission and Golgi fragmentation in midbrain neurons. *Neuroscience Letters, 720,* 134777. doi: 10.1016/j.neulet.2020.134777

Geraghty, R. J., Capes-Davis, A., Davis, J. M., Downward, J., Freshney, R. I., Knezevic, I., … Vias, M. (2014). Guidelines for the use of cell lines in biomedical research. *British Journal of Cancer, 111*(6), 1021–1046. doi: 10.1038/bjc.2014.166

Giguère, N., Delignat-Lavaud, B., Herborg, F., Voisin, A., Li, Y., Jacquemet, V., … Trudeau, L.-É. (2019). Increased vulnerability of nigral dopamine neurons after expansion of their axonal arborization size through D2 dopamine receptor conditional knockout. *PLOS Genetics, 15*(8), e1008352. doi: 10.1371/journal.pgen.1008352

Gitler, A. D., Dhillon, P., & Shorter, J. (2017). Neurodegenerative disease: Models, mechanisms, and a new hope. *Disease Models & Mechanisms, 10*(5), 499–502. doi: 10.1242/dmm.030205

Grosch, J., Winkler, J., & Kohl, Z. (2016). Early Degeneration of Both Dopaminergic and Serotonergic Axons – A Common Mechanism in Parkinson's Disease. *Frontiers in Cellular Neuroscience*, *10*. doi: 10.3389/fncel.2016.00293

Haddad, D., & Nakamura, K. (2015). Understanding the susceptibility of dopamine neurons to mitochondrial stressors in Parkinson's disease. *FEBS Letters*, *589*(24 0 0), 3702–3713. doi: 10.1016/j.febslet.2015.10.021

Heemels, M.-T. (2016). Neurodegenerative diseases. *Nature*, *539*(7628), 179. doi: 10.1038/539179a

Johnstone, A. D., Hallett, R. M., Léon, A. de, Carturan, B., Gibon, J., & Barker, P. A. (2018). A novel method for quantifying axon degeneration. *PLOS ONE*, *13*(7), e0199570. doi: 10.1371/journal.pone.0199570

Jouhilahti, E.-M., Peltonen, S., & Peltonen, J. (2008). Class III β-Tubulin Is a Component of the Mitotic Spindle in Multiple Cell Types. *Journal of Histochemistry and Cytochemistry*, *56*(12), 1113–1119. doi: 10.1369/jhc.2008.952002

Juárez Olguín, H., Calderón Guzmán, D., Hernández García, E., & Barragán Mejía, G. (2015, December 6). The Role of Dopamine and Its Dysfunction as a Consequence of Oxidative Stress [Review Article]. doi: https://doi.org/10.1155/2016/9730467

Kim, J.-Y., Yi, E.-S., Lee, H., Kim, J.-S., Jee, Y.-S., Kim, S.-E., … Ko, I.-G. (2020). Swimming Exercise Ameliorates Symptoms of MOG-Induced Experimental Autoimmune Encephalomyelitis by Inhibiting Inflammation and Demyelination in Rats. *International Neurourology Journal*, *24*(Suppl 1), S39-47. doi: 10.5213/inj.2040156.078

Koch, J. C., Bitow, F., Haack, J., d'Hedouville, Z., Zhang, J.-N., Tönges, L., … Lingor, P. (2015). Alpha-Synuclein affects neurite morphology, autophagy, vesicle transport and axonal degeneration in CNS neurons. *Cell Death & Disease*, *6*(7), e1811–e1811. doi: 10.1038/cddis.2015.169

Lesort, M., Terro, F., Esclaire, F., & Hugon, J. (1997). Neuronal APP accumulates in toxic membrane blebbings. *Journal of Neural Transmission*, *104*(4), 497–513. doi: 10.1007/BF01277667

Llobet Rosell, A., & Neukomm, L. J. (n.d.). Axon death signalling in Wallerian degeneration among species and in disease. *Open Biology*, *9*(8), 190118. doi: 10.1098/rsob.190118

Lobo, V., Patil, A., Phatak, A., & Chandra, N. (2010). Free radicals, antioxidants and functional foods: Impact on human health. *Pharmacognosy Reviews*, *4*(8), 118–126. doi: 10.4103/0973-7847.70902

Lodish, H., Berk, A., Zipursky, S. L., Matsudaira, P., Baltimore, D., & Darnell, J. (2000). *Molecular Cell Biology* (4th ed.). W. H. Freeman.

Lu, X., Kim-Han, J. S., Harmon, S., Sakiyama-Elbert, S. E., & O'Malley, K. L. (2014). The Parkinsonian mimetic, 6-OHDA, impairs axonal transport in dopaminergic axons. *Molecular Neurodegeneration*, *9*, 17. doi: 10.1186/1750-1326-9-17

Luo, S. X., & Huang, E. J. (2016). Dopaminergic Neurons and Brain Reward Pathways: From Neurogenesis to Circuit Assembly. *The American Journal of Pathology*, *186*(3), 478–488. doi: 10.1016/j.ajpath.2015.09.023

McDonald, W. M., Richard, I. H., & DeLong, M. R. (2003). Prevalence, etiology, and treatment of depression in Parkinson's disease. *Biological Psychiatry*, *54*(3), 363–375. doi: 10.1016/s0006-3223(03)00530-4

Riyahi, M., & Taherianfard, M. (2019). Motor defects, dopamine concentration and brain-derived neurotrophic factor in a rat model of Parkinson's disease can be affected by pre-infection with Toxoplasma gondii. *Physiol-Pharmacol*, *23*(4), 279–285.

Rosenthal, S. L., & Kamboh, M. I. (2014). Late-Onset Alzheimer's Disease Genes and the Potentially Implicated Pathways. *Current Genetic Medicine Reports*, *2*, 85–101. doi: 10.1007/s40142-014-0034-x

Salari, S., & Bagheri, M. (2019). In vivo, in vitro and pharmacologic models of Parkinson's disease. *Physiological Research*, *68*(1), 17–24. doi: 10.33549/physiolres.933895

Sasaki, Y., Vohra, B. P. S., Lund, F. E., & Milbrandt, J. (2009). Nicotinamide mononucleotide adenylyl transferase-mediated axonal protection requires enzymatic activity but not increased levels of neuronal nicotinamide adenine dinucleotide. *The Journal of Neuroscience: The Official Journal of the Society for Neuroscience*, *29*(17), 5525–5535. doi: 10.1523/JNEUROSCI.5469-08.2009

Scorziello, A., Borzacchiello, D., Sisalli, M. J., Di Martino, R., Morelli, M., & Feliciello, A. (2020). Mitochondrial Homeostasis and Signaling in Parkinson's Disease. *Frontiers in Aging Neuroscience*, *12*. doi: 10.3389/fnagi.2020.00100

Selkoe, D. J. (2001). Alzheimer's disease: Genes, proteins, and therapy. *Physiological Reviews*, *81*(2), 741–766. doi: 10.1152/physrev.2001.81.2.741

Sonne, J., Reddy, V., & Beato, M. R. (2020). Neuroanatomy, Substantia Nigra. In *StatPearls*. Treasure Island (FL): StatPearls Publishing. Retrieved from http://www.ncbi.nlm.nih.gov/books/NBK536995/

Sulzer, D., & Surmeier, D. J. (2013). Neuronal vulnerability, pathogenesis and Parkinson's disease. *Movement Disorders : Official Journal of the Movement Disorder Society*, *28*(1), 41–50. doi: 10.1002/mds.25095

Trist, B. G., Hare, D. J., & Double, K. L. (2019). Oxidative stress in the aging substantia nigra and the etiology of Parkinson's disease. *Aging Cell*, *18*(6), e13031. doi: https://doi.org/10.1111/acel.13031

Wang, W., Ma, C., Mao, Z., & Li, M. (2005). JNK inhibition as a potential strategy in treating Parkinson's disease. *Drug News & Perspectives*, *17*, 646–654. doi: 10.1358/dnp.2004.17.10.873916

Yaron, A., & Schuldiner, O. (2016). Common and Divergent Mechanisms in Developmental Neuronal Remodeling and Dying Back Neurodegeneration. *Current Biology: CB*, *26*(13), R628–R639. doi: 10.1016/j.cub.2016.05.025

Yarza, R., Vela, S., Solas, M., & Ramirez, M. J. (2016). C-Jun N-terminal Kinase (JNK) Signaling as a Therapeutic Target for Alzheimer's Disease. *Frontiers in Pharmacology*, *6*. doi: 10.3389/fphar.2015.00321

Zhang, X., Yin, M., & Zhang, M. (2014). Cell-based assays for Parkinson's disease using differentiated human LUHMES cells. *Acta Pharmacologica Sinica*, *35*(7), 945–956. doi: 10.1038/aps.2014.36

Zhong, H., & Yin, H. (2015). Role of lipid peroxidation derived 4-hydroxynonenal (4-HNE) in cancer: Focusing on mitochondria. *Redox Biology*, *4*, 193–199. doi: 10.1016/j.redox.2014.12.011

Zhou, F.-M., & Lee, C. R. (2011). Intrinsic and integrative properties of substantia nigra pars reticulata neurons. *Neuroscience*, *198*, 69–94. doi: 10.1016/j.neuroscience.2011.07.061